VII International Conference on Computational Methods for Coupled Problems in Science and Engineering
COUPLED PROBLEMS 2017
M. Papadrakakis, E. Oñate and B. Schrefler (Eds)

SIMULATION OF MACROSEGREGATION BENCHMARK ON A NON-UNIFORM COMPUTATIONAL NODE ARRANGEMENT WITH A MESHLESS METHOD

VANJA HATIĆ[*] AND BOŽIDAR ŠARLER[*] [†]

[*] Institute of Metals and Technology
Lepi pot 11, 1000 Ljubljana, Slovenia
e-mail: vanja.hatic@imt.si, web page: http://www.imt.si

[†] University Ljubljana, Faculty of Mechanical Engineering
Aškerčeva 6, 1000 Ljubljana, Slovenia
Email: bozidar.sarler@fs.uni-lj.si - Web page: http://www.fs.uni-lj.si

Key words: macrosegregation benchmark, columnar solidification, segregation prediction, meshless method, diffuse approximate method.

Abstract. An application of a meshless numerical method on a macrosegregation benchmark case is developed in the present paper. The test case is solidification in 2D rectangular cavity, filled with liquid metal and chilled from both sides. This is a highly non-linear problem due to a strong coupling of the macroscopic transport equations with the microsegregation model. The main result is the macrosegregation pattern of the solidified metal Al4.5wt%Cu alloy is used for evaluation of the problem. The model uses diffuse approximate meshless method with the second-order polynomial basis for spatial integration and explicit time-stepping. Simulations are performed on uniform and non-uniform computational node arrangements and compared to each other. The results on uniform and non-uniform node arrangements show a very good matching with the finite volume method results and results based on radial basis function collocation method. This shows that diffuse approximate method based on non-uniform node arrangements can be used for solving macrosegregation problems.

1 INTRODUCTION

Macrosegregation is a chemical inhomogeneity of the composition on the macro-scale level [1]. It is an undesired consequence of solidification and one of the major casting defects. Modelling of macrosegregation is therefore highly important for metallurgical and casting industries. Macrosegregation is a consequence of microsegregation, as during the solidification, the solute is pushed out from solid phase to the liquid phase (or vice versa). The solute is then transported from microscopic to macroscopic scale by the relative movement of the liquid and the solid phase in the transition region. There are different mechanisms which are connected with the macroscopic transport of solute. The main mechanisms are the convection-driven macrosegregation, shrinkage-driven macrosegregation, deformation driven macrosegregation, effect of floating grains, and effect of forced flow. Their magnitude and direction can work on different levels and in various directions.

The simulation of macrosegregation patterns is a complex, non-linear problem and involves solution of a coupled heat, mass and species transfer, phase change, and flow phenomena. Furthermore, the transport equations are coupled with the microsegregation model. One of the goals of our research group is to model macrosegregation for direct chill and low-frequency electromagnetic casting with a meshless method [2], [3]. The model for simulation of heat and momentum transfer for this kind of problems has already been developed [4]. The new meshless model for simulation of macrosegregation is in the process of development and is evaluated on a 2D test case, presented in this paper. The numerical benchmark is a 2D ingot solidification of a binary alloy, which has been proposed by Kosec et al. in [5]. In the paper authors presented results obtained with the classical finite volume method (FVM) [6] and meshless local radial basis function collocation method (LRBFCM) [7]. The same problem is solved by the diffuse approximate method (DAM) on a non-uniform node arrangement in the present paper. This is probably the first attempt to solve such kind of problems on non-uniform node arrangement.

2 MODEL FORMULATION

A volume-averaging method is used to model the transport equations. The method assumes that the mushy zone consists of two phases without voids. Each phase is described on the microscopic scale. The conservation equations are therefore derived microscopically and along with the interface boundary conditions make an appropriate description of the solidification process. The averaging of the equations over the representative elementary volume (REV), results in a model that can be used for solving practical problems.

The equations for simulation of the benchmark are simplified to the largest possible degree in order to enable easier comparison of different numerical procedures. The liquid phase is modelled as an incompressible Newtonian fluid. Laminar flow is assumed. Model assumes that the solid and the liquid densities are constant and equal for each phase. The buoyancy effect of density differences is modelled with the Boussinesq approximation. The solid phase is static. The mushy zone is modelled with the Kozeny-Carman relation for the porous flow. The dynamic viscosity of the liquid is assumed to be constant. The diffusion of the species conservation equation on the macroscopic level is neglected for both phases. Local thermal equilibrium is assumed in REV. The thermal conductivity and the specific heat capacity are assumed constant and equal in both phases. The lever rule is used to calculate the liquid volume fraction.

The following macroscopic equations are employed in the model [5]:

$$\nabla \cdot \mathbf{v} = 0, \tag{1}$$

$$\rho \frac{\partial \mathbf{v}}{\partial t} + \frac{\rho}{f_l} \mathbf{v} \cdot \nabla \mathbf{v} = -f_l \nabla p + \nabla \cdot \left(\mu \nabla \mathbf{v} \right) + f_l \mathbf{b} + f_l \frac{\mu}{K} \mathbf{v} ; \tag{2}$$

$$K = K_0 \frac{f_l^3}{\left(1 - f_l\right)^2} ; \; \mathbf{b} = \rho \left(1 - \beta_T \left(T - T_{\text{ref}}\right) - \beta_C \left(C_l - C_{\text{ref}}\right)\right) \mathbf{g} ,$$

$$\rho\frac{\partial h}{\partial t}+\rho\mathbf{v}\cdot\nabla h_l=\nabla\cdot\left(\lambda\nabla T\right), \tag{3}$$

$$\frac{\partial C}{\partial t}+\mathbf{v}\cdot\nabla C_l=0, \tag{4}$$

where t is time, $\mathbf{v}$ is the mixture velocity, ρ is the density, f_l is the liquid volume fraction, p is the pressure, μ is the dynamic viscosity, K_o is the Darcy constant, β_T and β_c are the temperature and concentration volume expansion coefficients, respectively, T is temperature, T_{ref} is the reference temperature, C_l is the liquid concentration, C_{ref} is the reference concentration, $\mathbf{g}$ is the gravity acceleration vector, h is the mixture enthalpy, h_l is the liquid enthalpy, λ is the mixture thermal conductivity, and C is the mixture concentration.

The following microscopic relations are used to calculate the macroscopic values [5]:

$$\mathbf{v}=\mathbf{v}_l f_l, \tag{5}$$

$$h=c_p T+L_f, \tag{6}$$

$$C=\left[f_l+\left(1-f_l\right)k_p\right]C_l, \tag{7}$$

$$T=T_f+m_l C_l. \tag{8}$$

where L_f is the latent heat of fusion, k_p is the partition coefficient, c_p is the specific heat capacity, T_f is the fusion temperature of pure metal, and m_l is the liquidus slope. Note that the equations (3) and (6) are different then in [5] as there was a misprint in the original paper.

3 NUMERICAL BENCHMARK DEFINITION

The geometry of the benchmark case represents a static ingot, with dimensions 2x2 cm, solidifying in a mould. The heat is extracted through the vertical walls. The top and the bottom walls are thermally insulated. The solidifying metal is Al4.5wt%Cu alloy, with the material properties given in Table 1. The duration of the simulation is 50 s.

The initial temperature and concentration are constant and set to 700 °C and4.5 wt%, respectively. The liquid metal is at rest at the beginning of the simulation. The geometry and the boundary conditions are symmetrical along the y axis, therefore only the right half of the ingot solidification is modelled. The symmetry boundary conditions are imposed for all fields on the west boundary. Dirichlet type boundary condition with boundary value equal to 4.5 wt% is imposed for concentration field on the remaining boundaries. The no-slip boundary condition is imposed on the remaining boundaries for the velocity field. The north and south boundaries are thermally insulated and the temperature gradient in the normal direction is equal to zero in these boundary nodes. The east, cooled boundary, is modelled with Fourier type of boundary condition, where the heat transfer coefficient is equal to 500 W/m^2/K and the external temperature is equal to 20 °C.

Table 1: Material properties of the Al4.5wt%Cu alloy used in simulation.

Property	Symbol	Unit	Value
Specific heat capacity	c_p	J/kg/K	$1\ 10^3$
Thermal conductivity	λ	W/m/K	$1.92\ 10^2$
Density	ρ	kg/m^3	$2.45\ 10^3$
Dynamic viscosity	μ	kg/m/s	$1.2\ 10^{-3}$
Gravity acceleration	g	m/s^2	9.80
Darcy constant	K_0	m^2	$5.56\ 10^{-11}$
Latent heat	L_f	J/kg	$4.00\ 10^5$
Fusion temperature	T_f	°C	660.00
Eutectic temperature	T_e	°C	548.00
Eutectic concentration	C_e	wt%	32.60
Liquidus slope	m_l	°C/wt%	-3.43
Partition coefficient	k_p	-	0.173
Thermal expansion coefficient	β_T	1/K	$1.3\ 10^{-4}$
Solutal expansion coefficient	β_C	1/wt%	$-7.3\ 10^{-3}$
Reference temperature	T_{ref}	°C	465.00
Reference concentration	C_{ref}	wt%	4.50

4 MESHLESS NUMERICAL PROCEDURE

A meshless numerical approach is used to perform the spatial discretization. Meshless methods [2], [3] have been in development in the recent decades and have already been applied to a wide range of physical problems [7]–[12]. The main benefit of the meshfree methods is that they do not require generation of elements, which are connected together by nodes in a complex predefined procedure, as it is the case with the classical numerical methods. The computational node arrangement can instead be created with less care. The computational nodes can be unstructured, which enables straightforward coping with irregular and more complicated computational domains [13].

4.1 Diffuse approximate method

Out of many available meshless methods, the diffuse approximate method [4], [8], [9], [13] is used to calculate the presented results. The weighted least squares are used to determine locally smooth and differentiable approximation of discrete data given in the computational nodes. The approximation $\hat{f}^k$ in the chosen node k is evaluated with the following expression:

$$\hat{f}^k(\mathbf{x}) = \mathbf{p}(\mathbf{x}, \mathbf{x}_k)\boldsymbol{\alpha}^k = \sum_{j=1}^{m} p_j(\mathbf{x}, \mathbf{x}_k)\alpha_j{}^k , \tag{9}$$

where $\mathbf{x}_k$ is the position vector of point k, $\mathbf{p}(\mathbf{x},\mathbf{x}_k)$ is the polynomial basis vector of order m and $\boldsymbol{\alpha}^k$ is the vector of coefficients. The quadratic polynomial base is used in the present simulations. The approximation of the solution (9) is obtained with the minimization of the expression:

$$J = \sum_{i=1}^{n} \theta(\mathbf{x}_i,\mathbf{x}) \left[f(\mathbf{x}_i) - \hat{f}(\mathbf{x}_i) \right]^2 , \tag{10}$$

where n is the number of nodes in the computational domain and θ is the Gaussian weighting function, which has a peak value of 1 at the chosen node k and is decreased with the Euclidian distance from this position. The vector of coefficients is obtained with solution of equation:

$$\sum_{i=1}^{n} \sqrt{\theta(\mathbf{x}_i,\mathbf{x}_k)}\mathbf{p}(\mathbf{x}_i,\mathbf{x}_k)\,\boldsymbol{\alpha}^k = \sum_{i=1}^{n} \sqrt{\theta(\mathbf{x}_i,\mathbf{x}_k)} f(\mathbf{x}_i) . \tag{11}$$

4.2 Space and time discretization

An explicit Euler time-stepping scheme is used for time integration. The time-step size is equal to 5 10^{-5} s and is chosen in accordance with the Courant-Friedrichs-Lewy and the Von Neumann stability conditions.

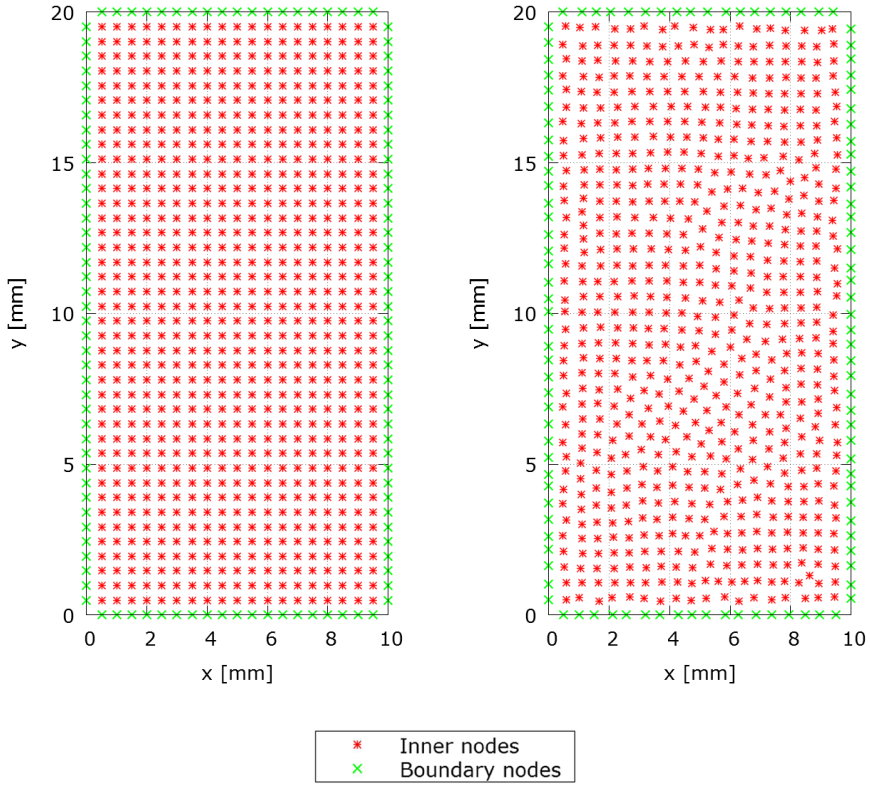

Figure 1: Examples of computational node arrangements used in simulations. Left : Uniform distribution with 878 nodes (21x41). Right : Non-uniform distribution with 754 nodes.

The evaluation of the conservation equations is performed locally. This means that the approximation is evaluated on a small portion of the global domain. Instead of using all the points (n), only a small amount of points (n_{loc}) is used for the approximation. Hence, each computational node of the global domain is assigned with its own local subdomain. The number of nodes in the local neighbourhood has to at least match the size of the basis vector, which is equal to 9 for the case of quadratic polynomial base. The solution (eq. 9) can be unstable for too small subdomains, if the nodes are arranged non-uniformly. Therefore, 13 nodded local neighbourhoods are used.

Two different computational node arrangements are used in simulations. The regular equidistant node arrangement is compared to the non-uniform node distribution. Sample distributions are shown on Figure 1. Simulations are performed on uniform distributions of two different densities 21x41 and 121x241. Non-uniform node distribution densities are chosen in such a way, that they roughly match the uniform ones.

4 RESULTS

The results are tabulated and compared to the finite volume and local radial basis function collocation method solution [5]. The final segregation pattern, after 50 s of simulation time is shown in Figure 2.

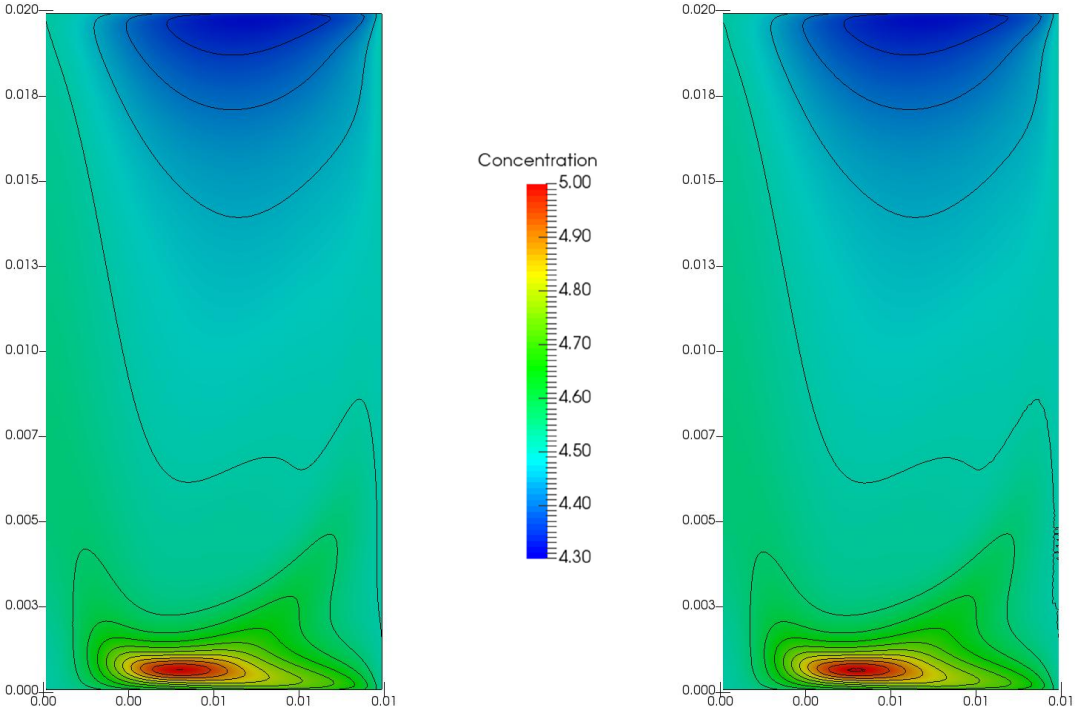

Figure 2: Macrosegregation pattern at the end of solidification for the computational node arrangement 121x241. The figure shows the concentration contour plot after 50 s of solidification. Left: results with the uniform distribution. Right: results with the non-uniform distribution.

The agreement with the reference results is tested in 66 reference points (see [5] for details on their positions) and is very good for both types of node distribution.The root-mean-square deviation, regarding the FVM, is equal to $1.99\ 10^{-3}$ for the uniform and $1.94\ 10^{-3}$ for the non-uniform distribution. The maximum relative difference is equal to $1.27\ 10^{-3}$ and $1.23\ 10^{-3}$ for the uniform and for the non-uniform node distribution, respectively.

As one can see the DAM application of the macrosegregation benchmark on the uniform and the non-uniform node distribution gives the results of the same quality. Furthermore, a comparison with the FVM and LRBFCM results show a very good agreement.

5 CONCLUSIONS

A meshless diffuse approximate method is applied to the 2D columnar solidification of a binary alloy benchmark problem. The simulations are performed on uniform and non-uniform computational node arrangements with different number of computational nodes. The results are compared to the solutions obtained by other methods [5]. DAM is for the first time used to calculate macrosegregation and the described benchmark. The results of the presented method are in a very good agreement with the other models. Furthermore, it is demonstrated that the solution is almost identical for calculations on uniform and non-uniform node distributions. The benchmark test is evaluated in order to confirm the basic model for segregation prediction, which includes only the effects of convection-driven macrosegregation. In the future, the model will be upgraded with the inclusion of the floating-grains effects and used to simulate macrosegregation in direct chill and low-frequency electromagnetic casting of aluminium-alloy billets.

ACKNOWLEDGEMENTS

This work was supported by the Slovenian Research Agency, grant number J2-7384 (BŠ) and the Young Researchers programme (VH).

REFERENCES

[1] Ludwig, A., Wu, M., and Kharicha, A. On Macrosegregation. *Metall. Mater. Trans* (2015) **A 46**:4854–4867.

[2] Liu, G.R. *Mesh Free Methods: Moving Beyond the Finite Element Method* . CRC Press (2009).

[3] Li, H., and Mulay, S.S. *Meshless Methods and Their Numerical Properties*. CRC Press (2013).

[4] Košnik, N., Guštin, A.Z., Mavrič, B., and Šarler, B. A multiphysics and multiscale model for low frequency electromagnetic direct-chill casting. *IOP Conf. Ser. Mater. Sci. Eng.* (2016) **117**:012052.

[5] Kosec, G., Založnik, M., Šarler, B., and Combeau, H. A meshless approach towards solution of macrosegregation phenomena. *Comput. Mater. Contin.* (2011) **22**:169–195.

[6] Založnik, M., and Šarler, B. Modeling of macrosegregation in direct-chill casting of aluminum alloys: Estimating the influence of casting parameters. *Mater. Sci. Eng.* (2005) **A413–414**: 85–91.

[7] Šarler, B., and Vertnik, R. Meshfree explicit local radial basis function collocation method for diffusion problems. *Comput. Math. Appl.* (2006) **51**:1269–1282.

[8] Sadat, H., and Prax, C. Application of the diffuse approximation for solving fluid flow and heat transfer problems. *Int. J. Heat Mass Transf.* (1996) **39**:214–218.
[9] Amaouche, M., Bouda, F.N., and Sadat, H. The onset of thermal instability of a two-dimensional hydromagnetic stagnation point flow. *Int. J. Heat Mass Transf.* (2005) **48**:4435–4445.
[10] Šarler, B. A radial basis function collocation approach in computational fluid dynamics. Cmes-Comput. *Model. Eng. Sci.* (2005) **7**:185–193.
[11] Kosec, G., and Šarler, B. Solution of a low Prandtl number natural convection benchmark by a local meshless method. *Int. J. Numer. Methods Heat Fluid Flow* (2013) **23**:189–204.
[12] Vertnik, R., and Šarler, B. Solution of a continuous casting of steel benchmark test by a meshless method. *Eng. Anal. Bound. Elem.* (2014) **45**:45-61.
[13] Hatić, V., Mavrič, B., and Šarler, B. Simulation of direct chill casting under the influence of low frequency electromagnetic field. *Proceedings of the 25th Anniversary International Conference on Metallurgy and Materials* (2016) p. 62.